NASA Technical Memorandum 108519

Verification of Orthogrid Finite Element Modeling Techniques

B.E. Steeve

October 1996

NASA Technical Memorandum 108519

Verification of Orthogrid Finite Element Modeling Techniques

B.E. Steeve
Marshall Space Flight Center • MSFC, Alabama

National Aeronautics and Space Administration
Marshall Space Flight Center • MSFC, Alabama 35812

October 1996

TABLE OF CONTENTS

LIST OF ILLUSTRATIONS

TECHNICAL MEMORANDUM

VERIFICATION OF ORTHOGRID FINITE ELEMENT MODELING TECHNIQUES

INTRODUCTION

Orthogrid structures are often used as a secondary mounting structure in aerospace designs where a regular to semiregular rectangular hole pattern is desired. Orthogrids are a strong, stiff, and relatively lightweight design solution. To maximize the stiffness while keeping the weight of an orthogrid structure low, I-beam sections are commonly used.

The stress analysis of such a structure is often performed using the finite element method. When creating a finite element model of an orthogrid structure, there are several possible techniques of varying complexity that can be employed. These range from a simple beam model to a full-blown solid element model. The choice of what technique to use depends on the availability of manpower, computer resources, and the desired level of results, both in accuracy and detail. This report looks at three modeling options and compares the results to experimental data.

ORTHOGRID

An orthogrid structure with I-beam sections is shown in figure 1. The structure is essentially two series of I-beams running orthogonal to each other and intersecting at nodes. Components are usually mounted to the orthogrid at these nodes.

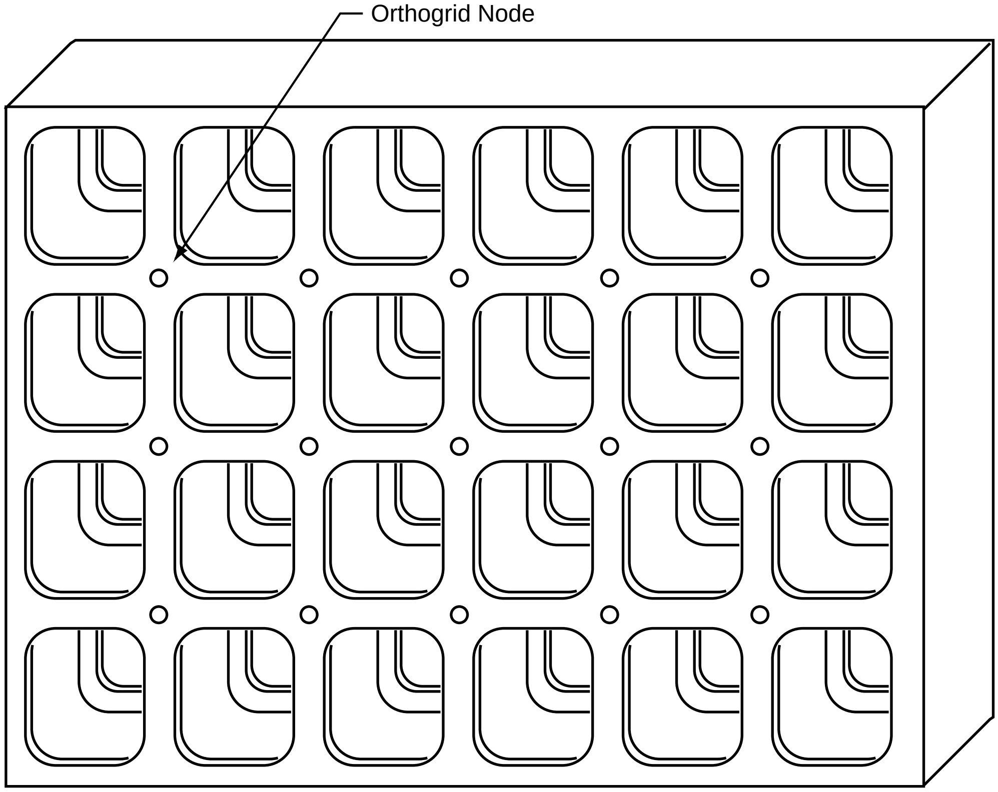

Figure 1. I-beam orthogrid structure.

FINITE ELEMENT MODELING

A finite element model of an orthogrid structure can be constructed using several different techniques. Three techniques are investigated here. Each one possesses a significantly different level of complexity. All of the finite element modeling was performed using the ANSYS 5.1 program.

Beam Model

The simplest model, shown in figure 2, is constructed entirely of beam elements. The element properties are those of the I-beam section (fig. 3). The elements connect at a single node at each orthogrid node. The element properties do not vary to account for the change of the I-beam section around the orthogrid nodes.

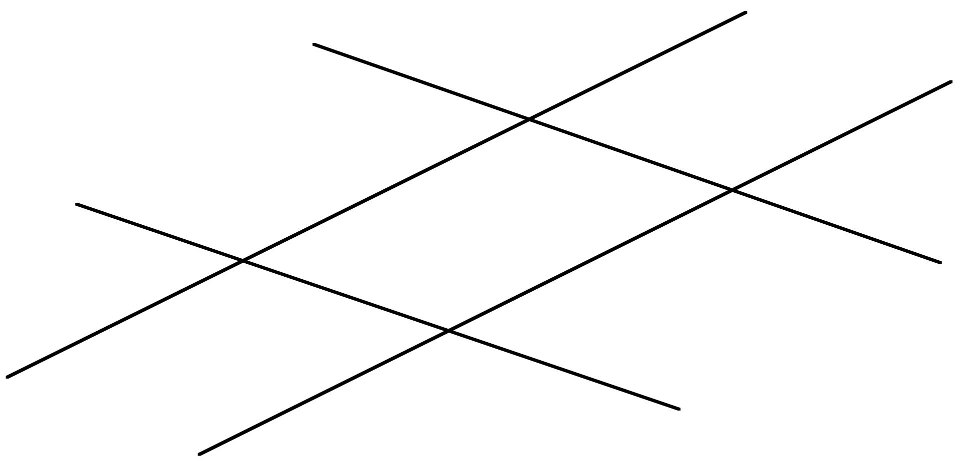

Figure 2. Beam element orthogrid model.

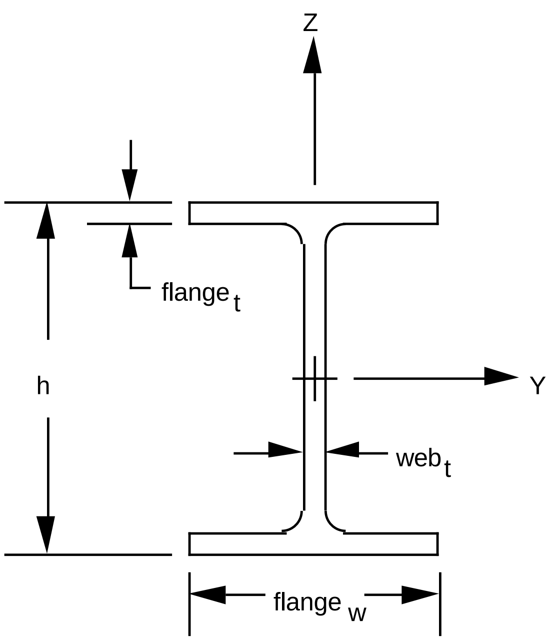

$$A = (h-2*flange_t)*web_t+2*flange_t*flange_w$$

$$I_{YY} = 1/12*web_t*(h-2*flange_t)^3+ 2*(1/12*flange_w*flange_t^3+ flange_w*flange_t*((h-flange_t)/2)^2)$$

$$I_{XX} = 1/12*(h-2*flange_t)*web_t^3+ 2*(1/12*flange_t*flange_w^3)$$

Figure 3. I-beam cross section.

Shell and Beam Model

The next model, shown in figure 4, better represents the three-dimensional nature of the structure. It uses shell elements to model the web of the I-beam and offset beams to model the I-beam flanges. The beam elements have the same properties of an I-beam flange with the centroid of the flange offset from the node locations by one half of the flange thickness (fig. 5). Like the beam model, the I-beam section does not vary at the orthogrid nodes.

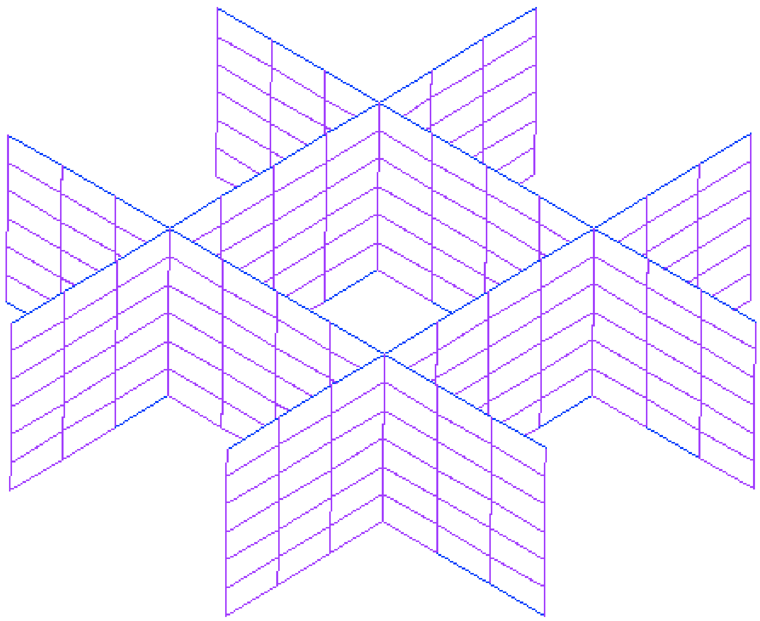

Figure 4. Beam and shell element orthogrid model.

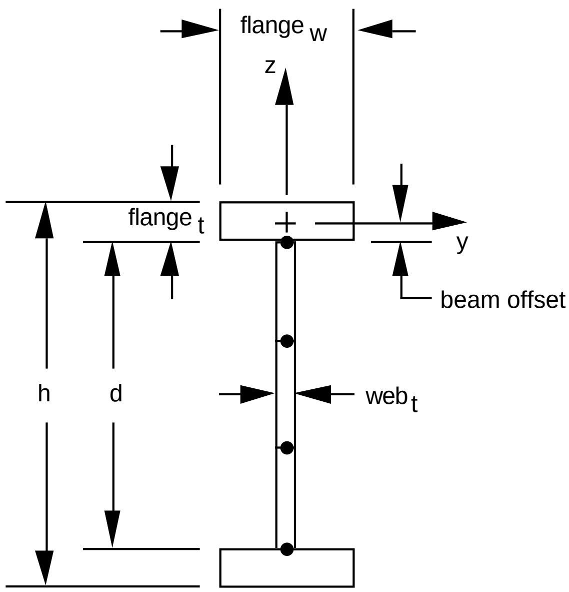

Figure 5. Beam and shell element representation of I-beam section.

Shell Model

The third model is built using all shell elements. This model better represents the effect of the nodes. The radius of the I-beam flanges around the nodes are modeled, and the increased thickness of the webs at the nodes is modeled by tapering the thickness of the web elements connected to the nodes to three times the nominal I-beam thickness (the value of three was chosen somewhat arbitrarily) (figs. 6 and 7).

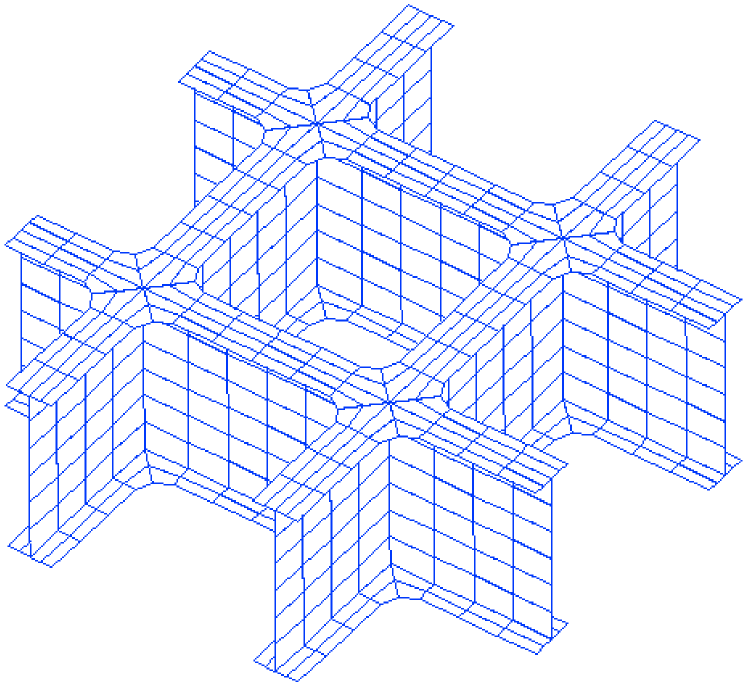

Figure 6. Shell element orthogrid model.

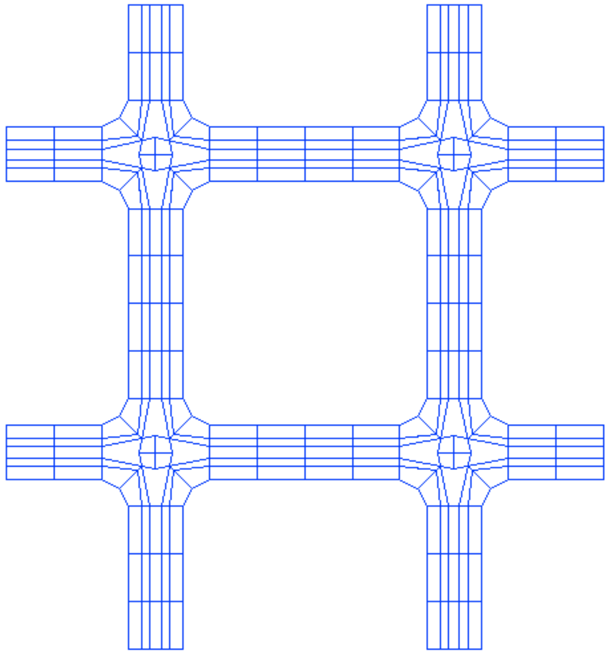

Figure 7. Shell element orthogrid model showing taper of web elements at each orthogrid node.

A drawback of this model is the overlap of the flange elements with the web elements (fig. 8). ANSYS does not have the capability to input an offset distance for shell elements from their node locations. Rigid elements could be used to create an offset, but this adds additional modeling complexity and were not used. Consequently, the I-beam section representation of this model is not entirely accurate. The moment of inertia, Iyy, can be matched with the actual I-beam inertia by adjusting the distance d (as was done in this investigation). This leaves the overall height slightly less than the actual height, which produces a lower maximum fiber stress on the top and bottom surfaces of the I-beam. In this investigation, the stress/strain values were about 2 percent less than what they should have been.

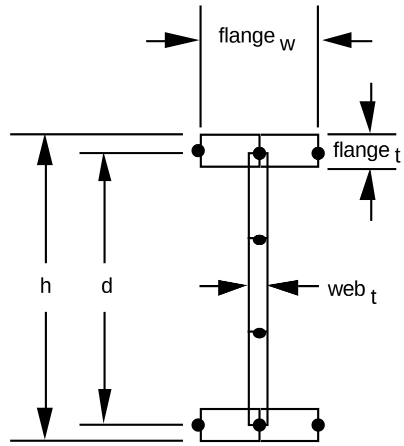

Figure 8. Shell element representation of I-beam section.

VERIFICATION

To check the accuracy of the various orthogrid modeling techniques, a test was performed to provide strain gauge data to compare with the finite element model predictions. An orthogrid panel was instrumented and then loaded in two different configurations. In one configuration, a load was applied normal to the panel and, in the other, an in-plane load was applied to the side of the panel. The setup for both configurations was designed so that the boundary conditions could be easily modeled.

Test Article

The orthogrid panel used in the test is shown in figure 9. All of the interior members were standard I-beam sections and the edges were rectangular sections. The section dimensions are listed in figures 10 and 11. The panel was constructed from a single plate of aluminum 2219.

Loads

The two loading configurations are shown in figures 12 and 13. In the first configuration, a 2,500-lb normal load was applied at three points in the center of the panel. The load line was positioned such that the load at the three application points were equal. The load was reacted through a single point at each corner.

In the second configuration, a 5,000-lb in-plane load was applied along two lines on one side of the panel. The load was reacted on the other side through a line at each end.

The loads were applied incrementally, with data taken at every increment.

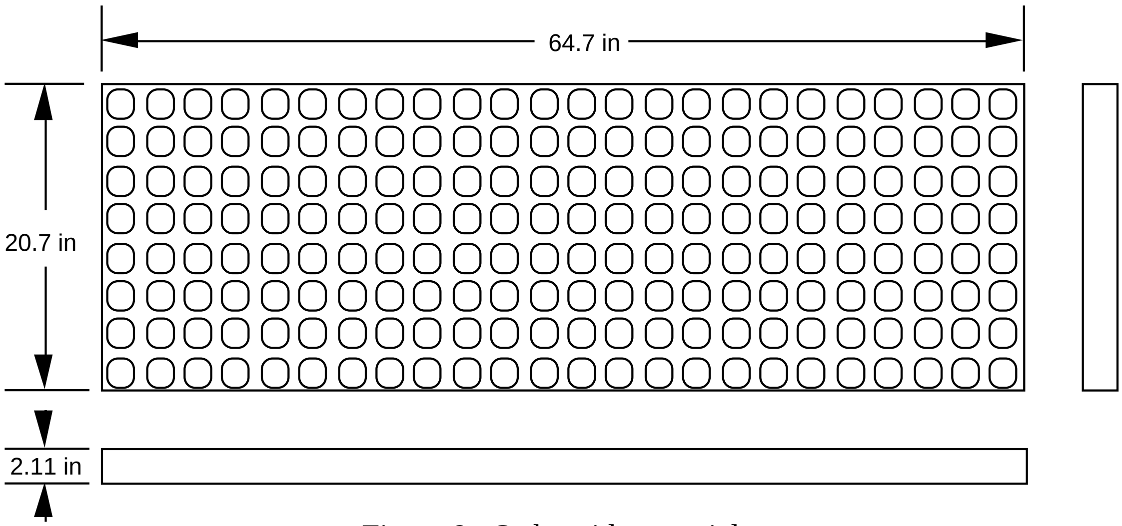

Figure 9. Orthogrid test article.

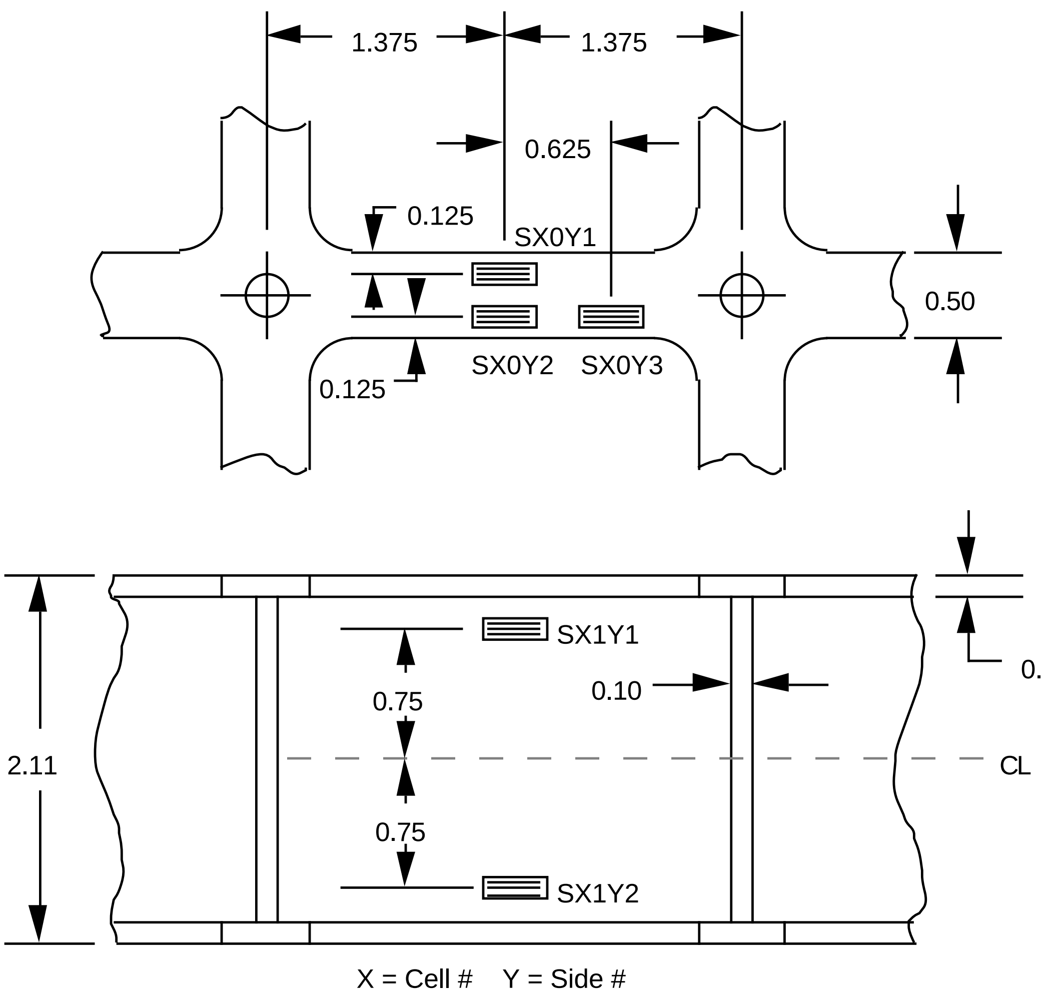

Figure 10. Typical strain gauge installation on interior members of orthogrid test article.

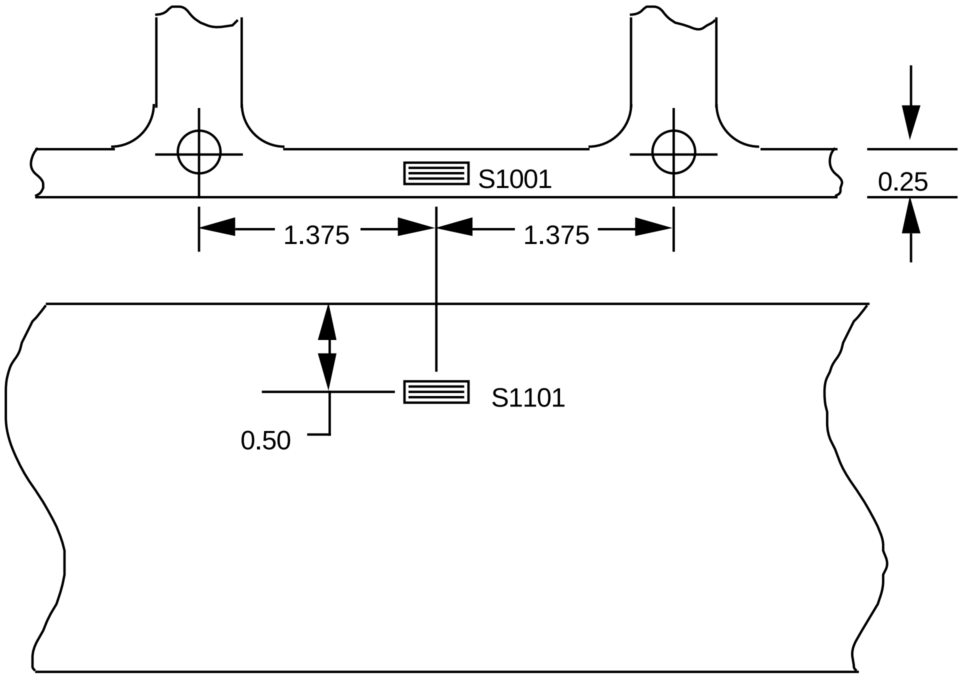

Figure 11. Strain gauge installation on side of orthogrid test article.

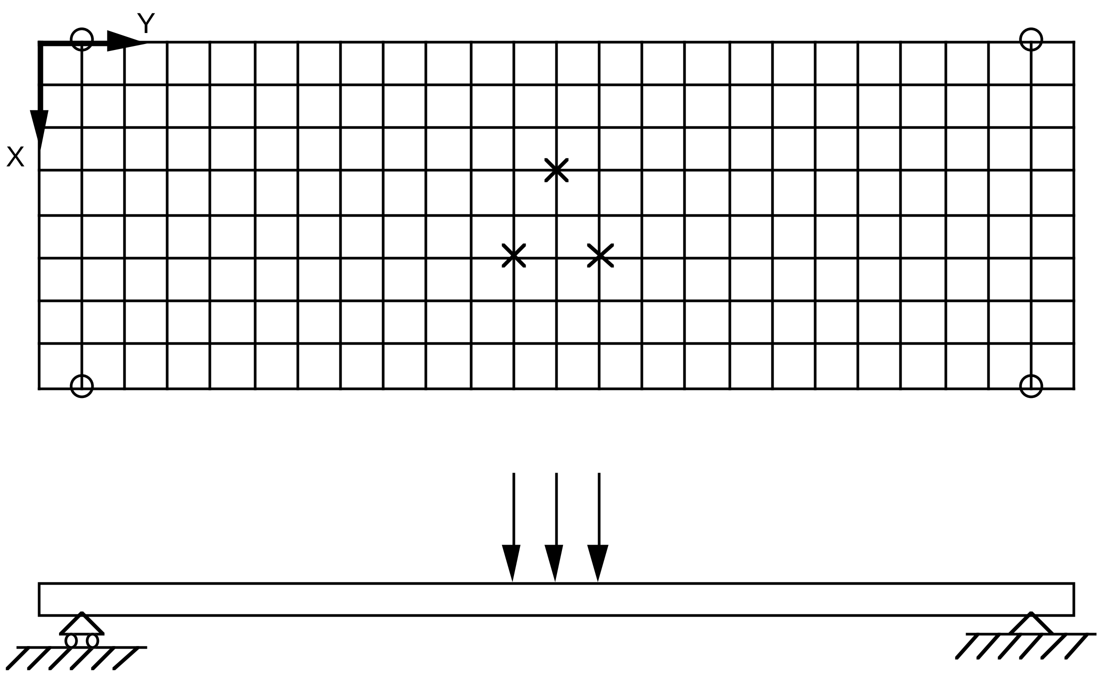

Figure 12. Normal load configuration.

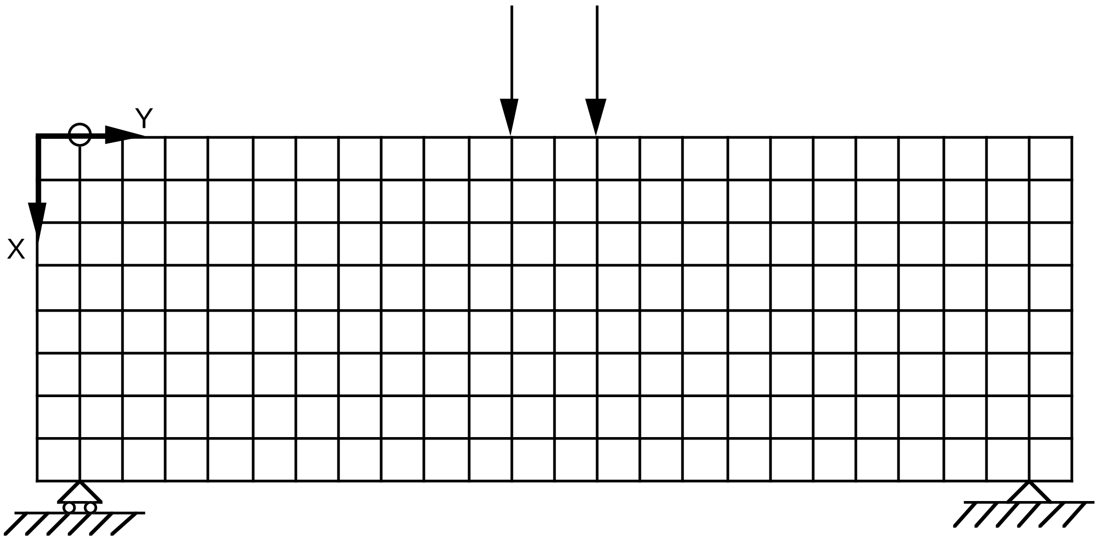

Figure 13. Side load configuration.

Instrumentation

Instrumentation of the test article included 32 strain gauges applied on the orthogrid members as shown in figure 14. The details of the gauge location on each member are shown in figures 10 and 11. The gauges were oriented to measure the axial strain of the I-beam sections.

Two deflection transducers measured the deflection for each load configuration. The points of each measurement are shown in figure 14.

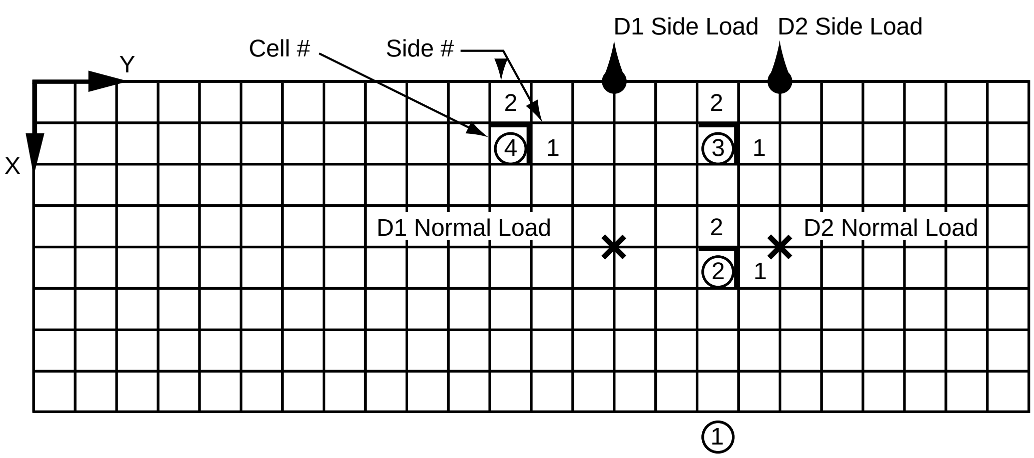

Figure 14. Locations of strain gauge and displacement instrumentation.

RESULTS

The results from the two tests, along with the predicted finite element results from the three models, are shown in figures 15 through 24. The incremental results indicate that the behavior of the panel was linear with respect to the loading. This is shown by the deflection charts, figures 15 and 16. The strain results, figures 17 through 24, are given for the final maximum loading.

Stiffness

The shell model was the only one that accurately predicted the deflection behavior of the test panel. This model was within 5 percent of the normal load deflection and within 8 percent of the side load deflection. The other two models, on the other hand, did a poor job of matching the test data. For the normal load configuration, the beam model was off by 20 percent and the beam and shell model was off by 16 percent. The predicted side load deflection was particularly poor, with both models off by more than 100 percent. In each configuration, the two models over-predicted the deflections, indicating they are considerably less stiff than the actual orthogrid panel.

The low stiffness of the beam and the beam and shell models can be accounted for by the way the orthogrid nodes were modeled, or rather not modeled. Both of these models were modeled essentially as constant section beams intersecting at a single node or line of nodes in the case of the beam and shell model. The effect of the extra material at each orthogrid node was not accounted for.

Strains

For the normal loading configuration, the highest strains occurred in the members running lengthwise. All of the models did reasonably well in matching the strain gauge data from these members. The beam and shell model matched the two midline I-beam flange gauges most accurately, within 2 percent. The off-midline gauge closer to the nodes, SX023, was best matched by the shell model, within 1 percent, which can be attributed to the higher fidelity of this model around the nodes.

The strains in the members running across the width were very low. The models varied greatly in how well they matched these strains. Since low-stressed areas are not critical design drivers, it is not very important that the models match the test values at these areas in order to assess their performance

For the side-loading configuration, the highest strains occurred in the off-midline flange gauge, SX023. The shell model most closely matched the strain at this location, within 6 percent. The other two models exceeded the test values by 20 to 40 percent. The strain values at the other gauge locations were fairly low and, again, the model predictions varied, with none matching very well.

CONCLUSIONS

Based on this study, the shell model does the best job predicting the deflection behavior of an orthogrid structure. The nodes have a significant effect on the behavior of an orthogrid structure, which the beam and beam and shell models do not capture. It may be possible to alter these two models by modifying the beam section around the nodes to better model this effect.

All three models do reasonably well predicting strains due to normal loading. For side loading, only the shell model performed well in predicting the strains. The other two models tended to over-predict the maximum strains in the flange by a significant amount. These two modeling techniques yield reasonable results between nodes but are conservative near the nodes.

This experiment shows that the best overall choice for modeling orthogrid is the shell element method. This is especially true where deflections and stiffness are important. However, when model size and analysis time are important, which is usually the case, both the beam and beam and shell element methods provide reasonable to conservative results for a stress analysis. If the hardware is such that capturing the three dimensional nature of the structure is not important or poses no modeling difficulties, then the beam element method is probably sufficient. When the thickness of an orthogrid structure is more important, such as when it has multiple interfaces to other hardware at different locations and planes, then the beam and shell element method will suffice.

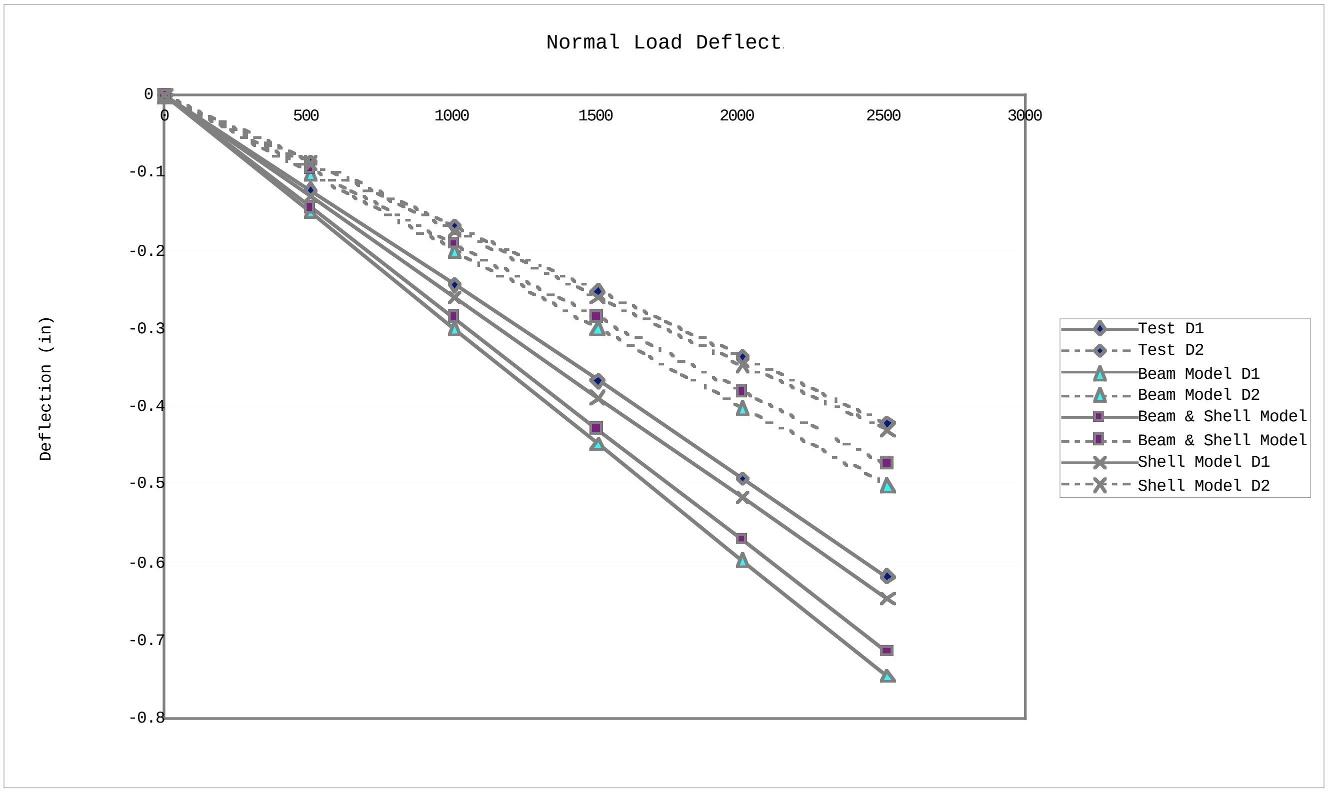

Figure 15. Normal load configuration deflection.

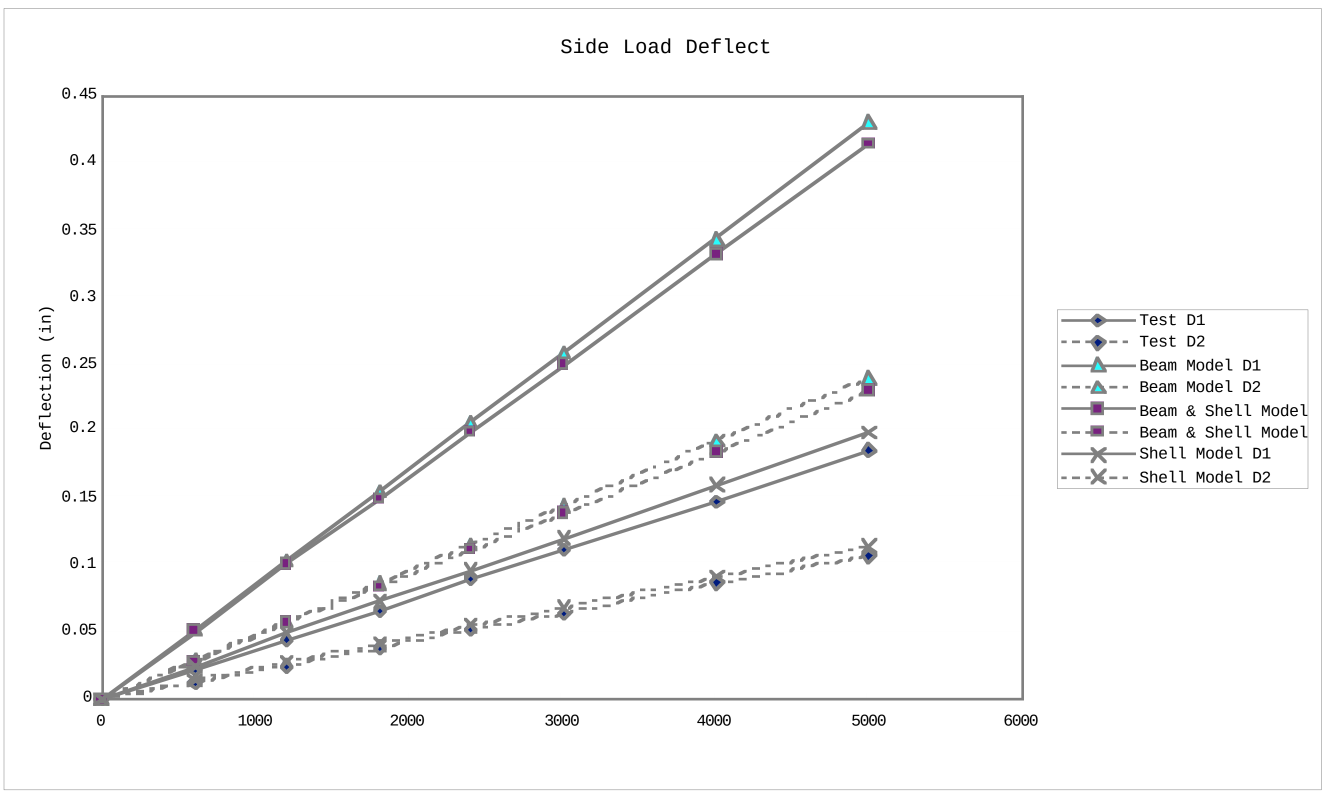

Figure 16. Side load configuration deflection.

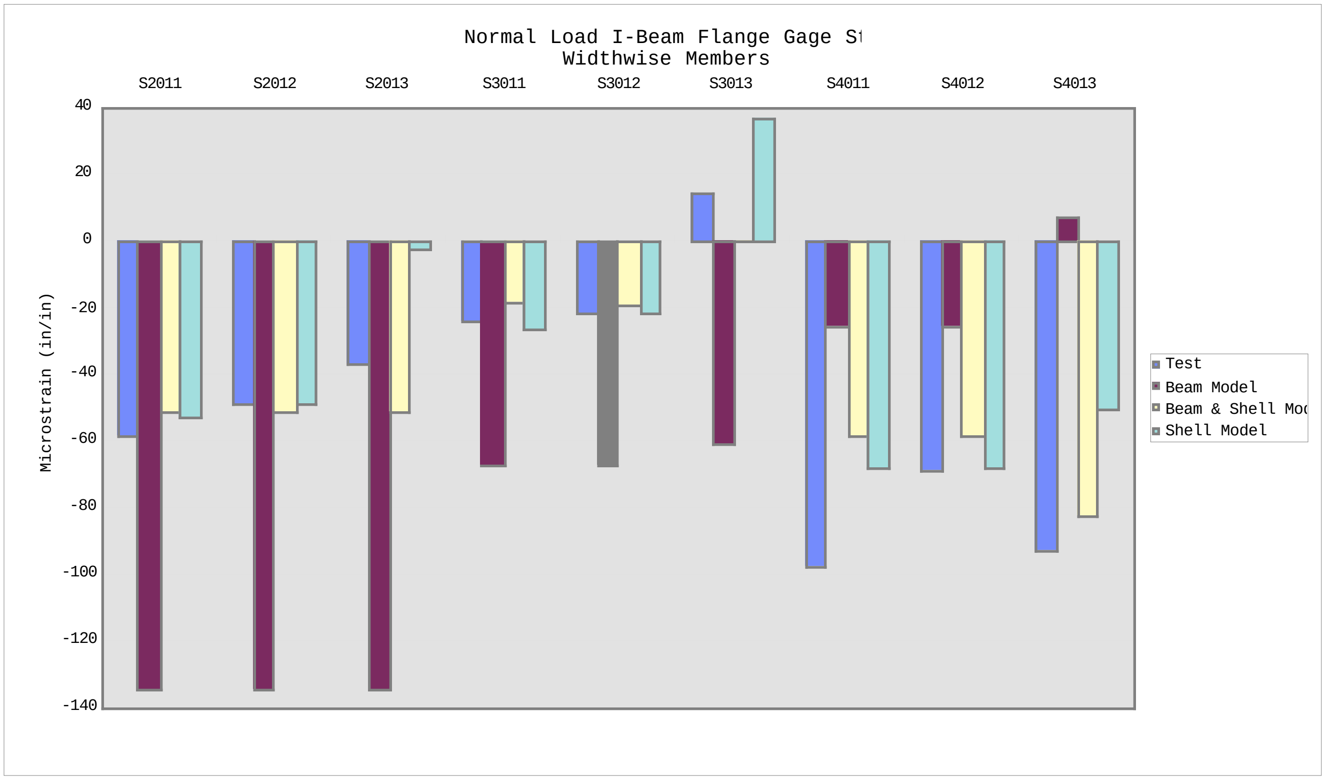

Figure 17. Normal load configuration I-beam flange strain on members running across width.

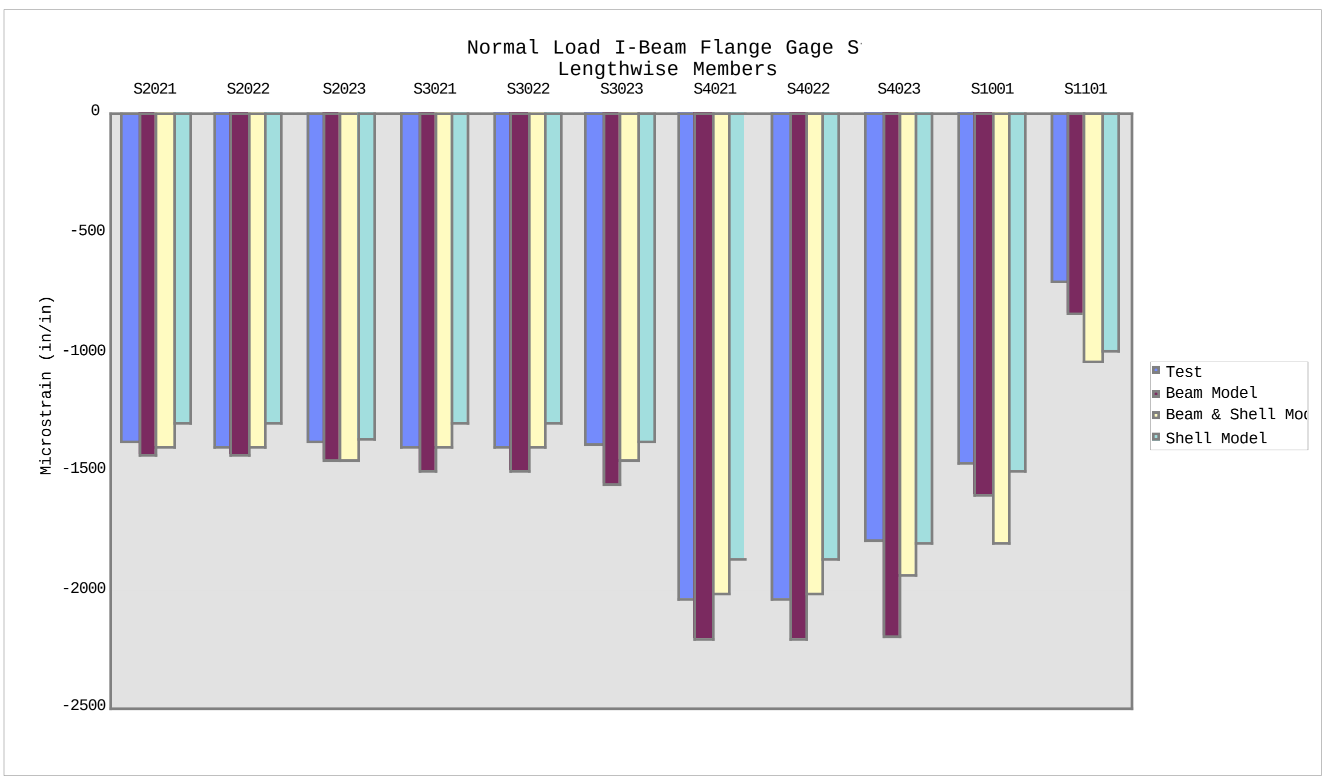

Figure 18. Normal load configuration I-beam flange strain on members running along length.

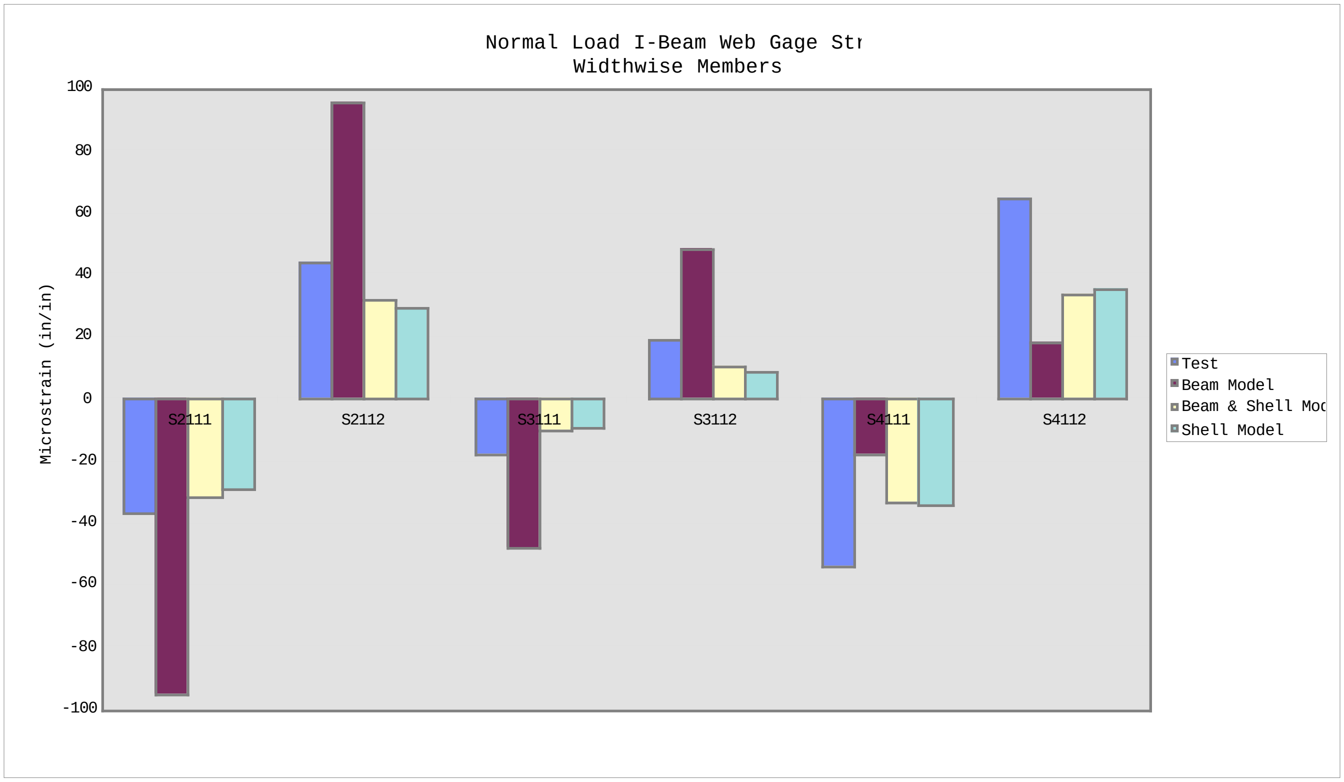

Figure 19. Normal load configuration web strain on members running across width.

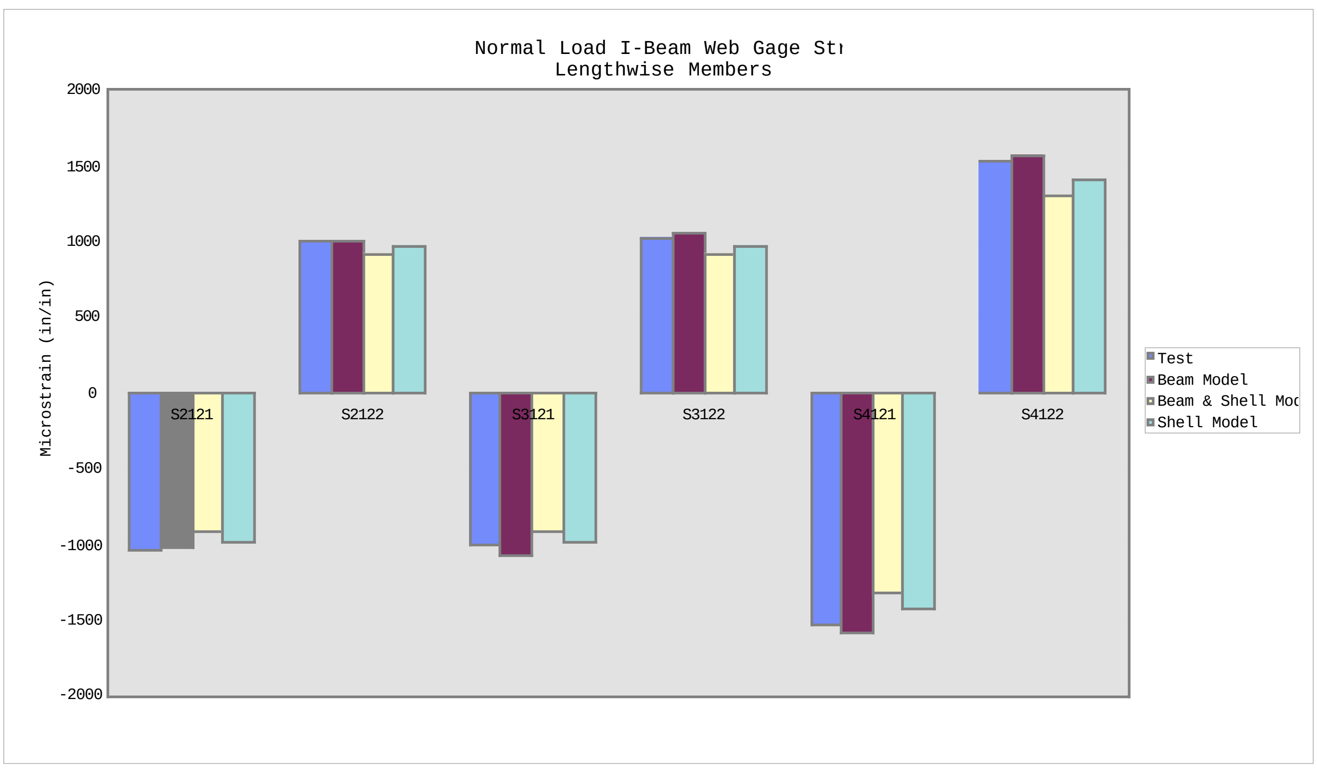

Figure 20. Normal load configuration web strain on members running along length.

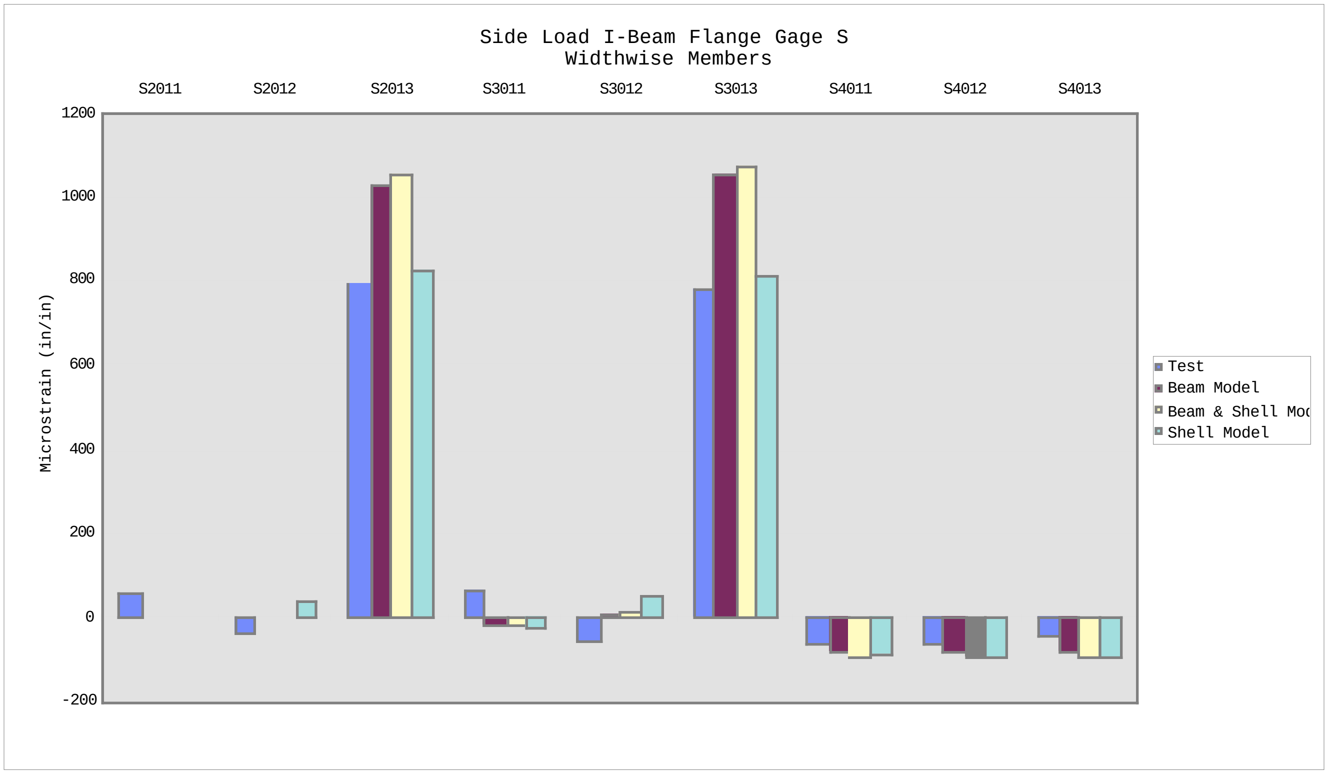

Figure 21. Normal load configuration I-beam flange strain on members running across width.

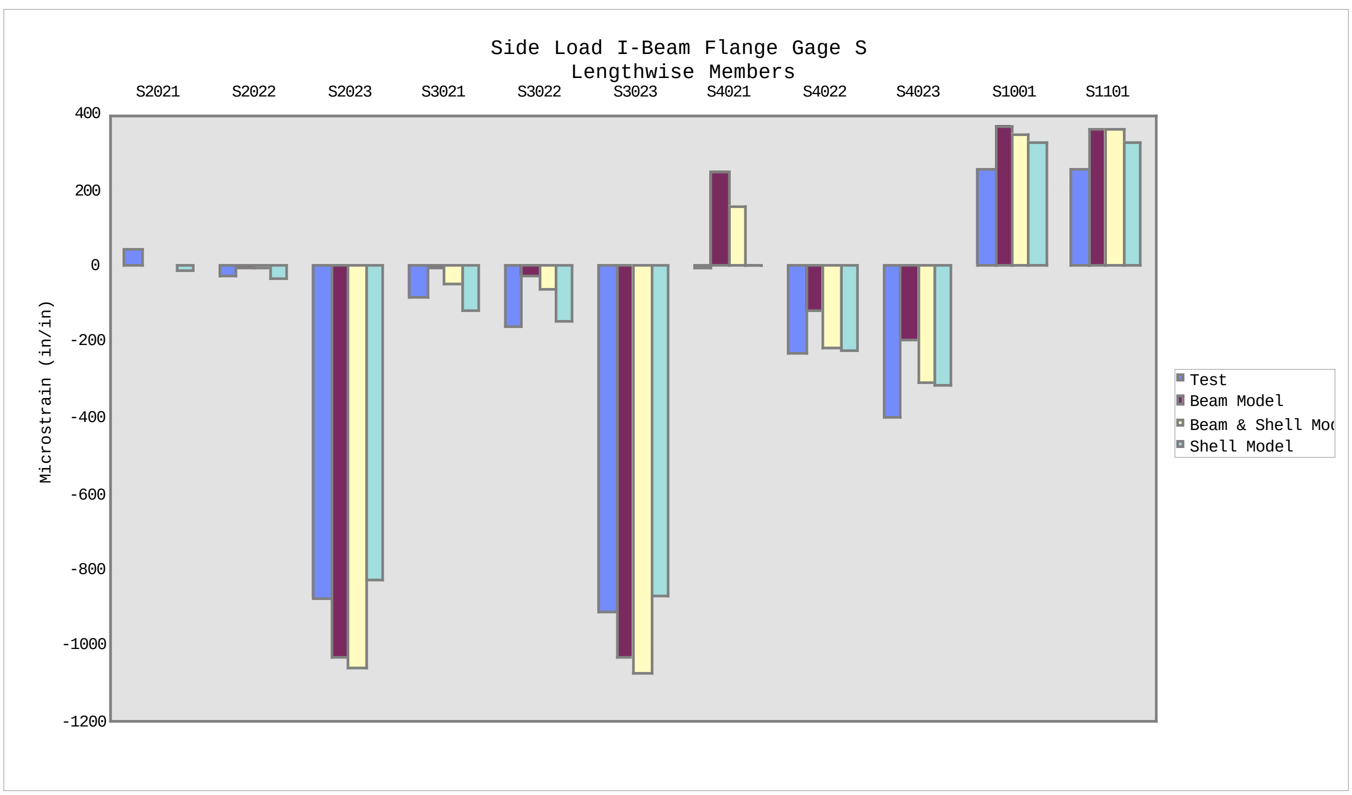

Figure 22. Normal load configuration I-beam flange strain on members running along length.

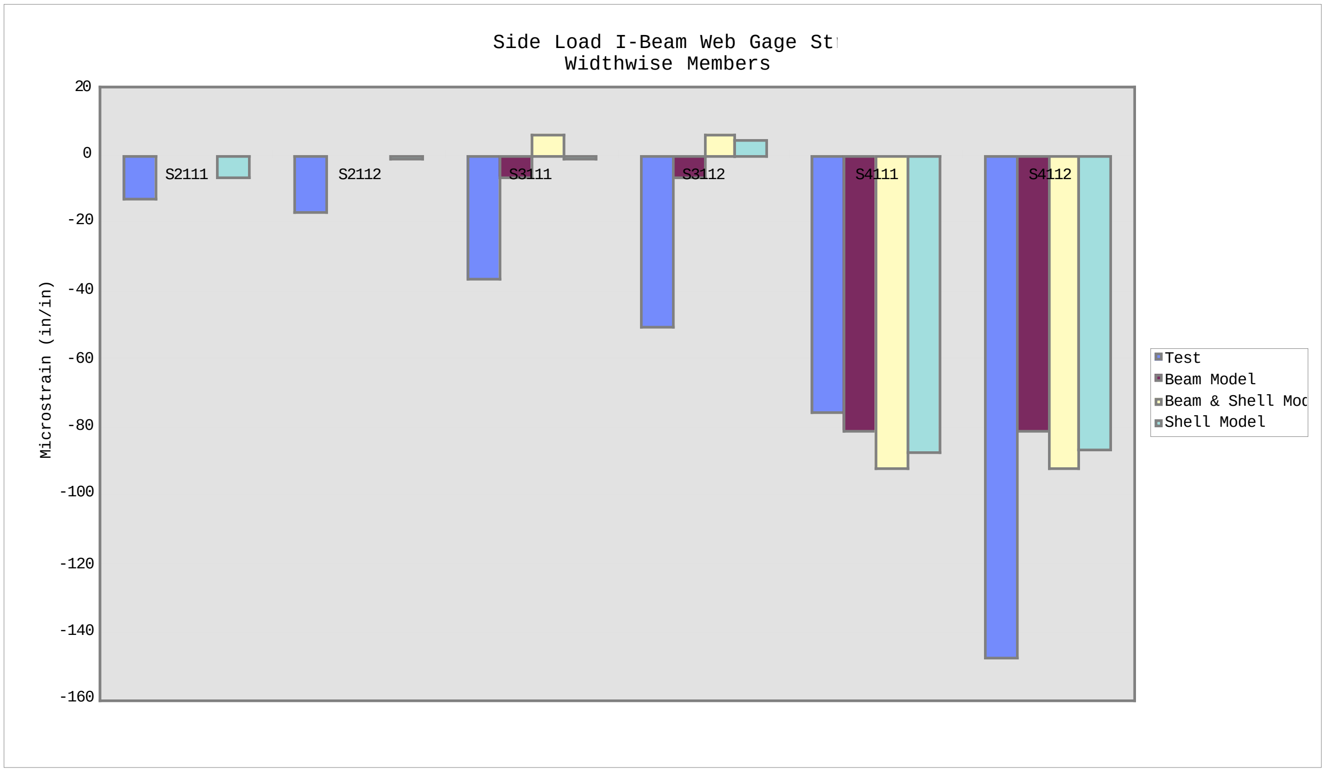

Figure 23. Normal load configuration web strain on members running across width.

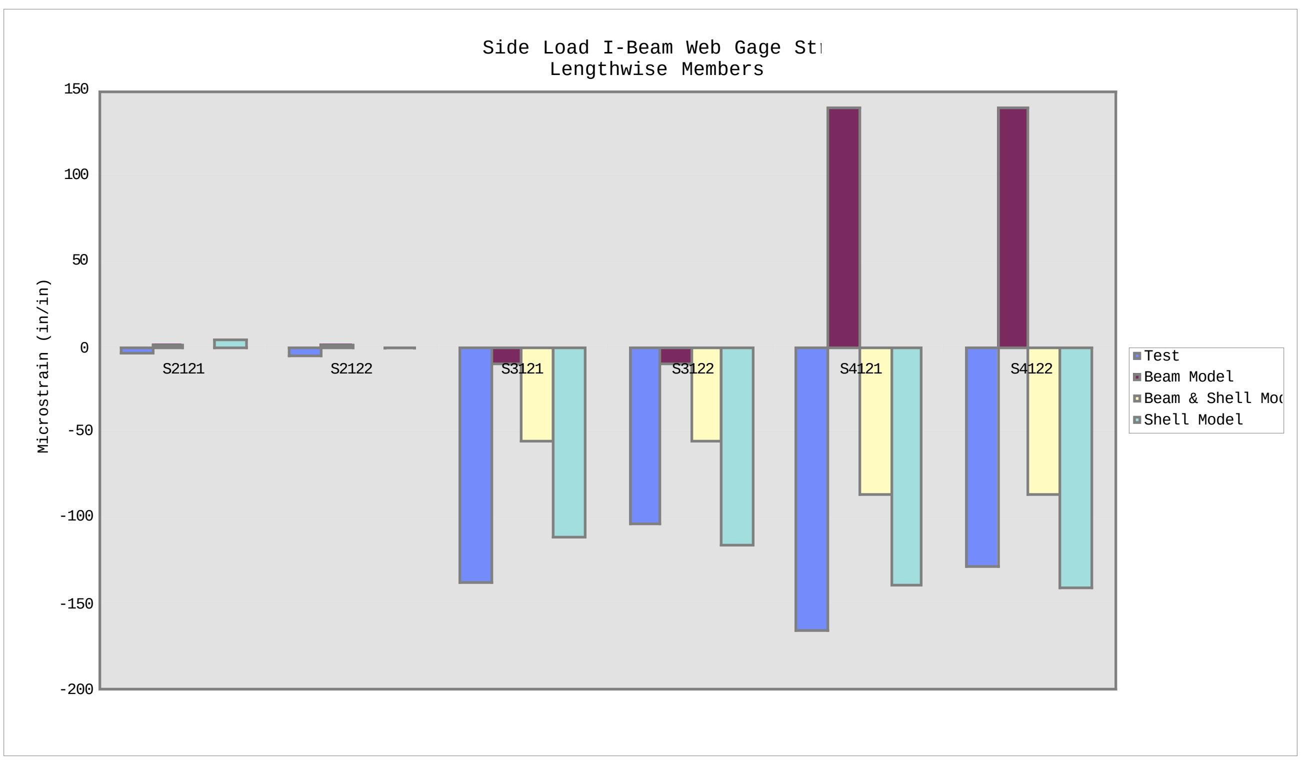

Figure 24. Normal load configuration web strain on members running along length.